DE GRUYTER OPEN
Slovak Journal of Civil Engineering Vol. 26, 2018, No. 3, 49 – 64
DOI: 10.2478/sjce-2018-0020

THE SEISMIC INVESTIGATION OF OFF-DIAGONAL STEEL BRACED RC FRAMES

Keyvan RAMIN[1*], Mahmoud R. MAHERI[2]

Abstract

Steel bracing may be used to enhance the seismic strength of RC frames. Concentric steel bracing generally reduces ductility, which is a key component of seismic design. To overcome the problem, ductile steel brace-RC frame systems are therefore usually introduced in the form of eccentric braces. In the present study, the Off-Diagonal Bracing System (ODBS), which works as a concentric type of bracing, is investigated. In this paper the response of ODBS elements to cyclic loading is first explored and compared with those of other types of bracing such as X-bracing and inverted-V bracing systems. The time history analysis responses and cyclic hysteresis responses of a number of low-rise to mid-rise RC frames retrofitted with different types of bracing systems are then evaluated and compared. It is shown that under seismic excitation, a much reduced base shear is experienced by frames retrofitted with ODBS compared to other bracing systems. The results of time history and cyclic hysteresis response analyses also indicate a far greater energy dissipation capacity and ductility for the ODBS compared to other bracing systems. It is also concluded that ODBS performs best in low-rise frames. The out-of-plane buckling response of the ODBS is also investigated, and it is shown that a double-plated central connection can control such an adverse response.

Address

[1] Ferdowsi University of Mashhad, College of Engineering, Dept. of Civil Engineering, Mashhad, Iran
[2] Shiraz University, Dept. of Civil Engineering, Shiraz, Iran

* ***Corresponding author:*** keyvan_ramin@yahoo.com

Key words

- ODBS,
- Concentric steel brace,
- Steel bracing,
- RC frame,
- Buckling,
- Hysteresis capacity,
- Time history analysis.

1 INTRODUCTION

Many existing reinforced concrete buildings were designed based on old codes of practice, now known to be inadequate in providing for the safety of buildings under seismic forces. Seismic retrofitting has therefore become a popular subject for investigation in recent years. There are many well-known seismic retrofitting methods for RC structures (A. K. Chopra, 2016). The steel bracing of RC frames is one of the more attractive methods in this regard. Steel bracing of RC frames can be applied either externally or internally. In external bracing, steel trusses or frames are attached to a frame's exterior (T. D. Bush et al., 1991). In internal bracing, steel bracing members are inserted inside individual unit frames that are concurrent with the axes of the frames. In this method, steel braces can be connected to RC frames either directly or indirectly. Earlier forms of internal bracing used intermediary steel frames inside concrete unit frames, and the bracing members were attached indirectly to the RC frame via these steel frames (H. Ohishi et al., 1988; Y. Tagawa et al., 1992). On the other hand, the steel braces in the direct connection method are directly connected to the RC frames without the use of an intermediary steel frame but with the aid of a gusset plate and connecting plates. Both the external bracing and indirect internal bracing systems, which were primarily developed as retrofitting measures, have some drawbacks, including architectural limitations, cost, and technical difficulties in attaching the brace system to the concrete frame. These considerations make the two systems less attractive compared to directly connected internal bracing.

Direct internal bracing can be used not only as a retrofitting system for existing buildings, but also as a shear-resisting element to be used in the seismic design of new buildings. Experimental and theoretical studies conducted by Maheri et al. (M. R. Maheri et al., 1995; 1997; 2003; 2008; H. Ghaffarzadeh et al.,2006), Tasnimi and Massomi (A. Tasnimi, et al., 1999), and Abou-Elfath and Ghobarah (A. Abou-Elfath et al., 2000) have shown that by using appropriate forms of direct internal bracing, it is possible to enhance the load-resisting capacity of RC frames and improve their seismic performance.

Two types of bracing configurations are commonly used, i.e., concentric and eccentric. Concentric bracing systems (e.g., X-bracing, Inverted-V, etc.) can be an attractive option because of the relative economy of their design and construction along with their sound strength-enhancing capacity and stiffness performance. However, they usually cause a reduction in a system's ductility, which is a key parameter in seismic performance. Eccentric bracing systems, on the other hand, lack the capabilities of concentric bracing regarding strength and stiffness but exhibit a somewhat more ductile performance. However, an off-diagonal bracing system (ODBS) is a concentric type system, which has the ductility capacity of an eccentric system. This is due to the fact that the nonlinear response of an ODBS is governed by two yielding stages. The first stage is the yielding of the corner (third) brace member, which is deliberately designed to be weaker to act as a fuse component and which is followed by the subsequent yielding of other members. Also, another advantage of ODBS is its ability to accommodate door and window openings.

Majidzamani et al. (S. Majidzamani, 2006) conducted an experimental study of full-scale off-diagonal braced frames. They concluded that by detailing the cross sections of brace members and their connections against out-of-plane buckling, all potential failure modes can be transferred to an in-plane buckling deformation. They also found that the inelastic flexure of brace members is the main source of energy dissipation in Y-braced frames (S. Majidzamani, 2006). Bazzaz et al. (M. Bazzaz et al., 2015) carried out a numerical investigation on a frame with an off-centre bracing system. They introduced a circular element in a bracing system to dissipate energy during cyclic loading. Their results showed that using a ductile element or circular energy dissipater for increasing ductility can be applied not only to off-centre bracing systems, but also to concentric bracing systems. Majidzamani et al. (S. Majidzamani et al., 2012) carried out another experimental investigation to study the behaviour of y-braced frames. In their investigation, quasi-static cyclic loading was applied to four full-scale, two-bay frames with y-bracings of various cross sections and connection types. The bays were braced symmetrically to have a combination of tensile and compressive braces at all the loading stages. Their results showed that out-of-plane buckling with a single curvature in braces can be substituted for in-plane, double curvature buckling through appropriate detailing of the cross sections and connections.

Retrofitting existing RC frames with steel bracing may increase demands on RC members such as beams, columns and foundations. Therefore, care must be taken to control new demands on members due to retrofitting. The possible increase in uplift is one side effect for a foundation (L. Lorenzo De Stefani, 2015). In a study reported by Majidzamani et al. (S. Majidzamani, 2011), they noted that y-bracings impose much less vertical uplift on foundations compared to X bracings. Large uplift forces on foundations due to seismic lateral loads are a disadvantage of X-braced frames. Installing y-bracing in two adjacent bays of a frame in a mirrored configuration could double the resisting lever arm, thereby halving the uplift force. They suggested that in ODBS, an increase in the post-buckling drift increases the damping ratio. At drift ratios of more than 0.02, the damping of Y-braced frames was reported to be comparable to that of X-braced frames, i.e., ranging between 20% and 25% (S. Majidzamani, 2011). Recently, Sedaghati et al. (P. Sedaghati et al., 2017) reported the results of a parametric investigation carried out on the response of ODBS. They noted that the pinching effect in hysteretic cycles of the ODBS with simple connections results in a smaller hysteresis loop area, which represents a lower energy dissipation capacity. On the other hand, an ODBS with rigid connections provides higher energy dissipation capacity because of their greater hysteresis loop area. They also concluded that the optimal range of eccentricity in an ODBS with simple connections is 0.25 < e1 < 0.4, while in an ODBS with rigid connections, it is 0.5 < e1 < 0.7.

Despite the above studies, the actual earthquake time history response of ODBS in comparison with other, more common forms of bracing systems, including those reported in (K. Ramin et al., 2015), have not been fully investigated. In the following, the design basis for ODBS is first discussed. The response of ODBS elements to cyclic loading is then compared with those of other types of bracing such as X-bracing and inverted-V bracing systems. The time history response and cyclic response of a number of low-rise to mid-rise RC frames retrofitted with different types of bracing systems are also explored and compared.

2 ODBS DESIGN BASIS

The ODBS is a three-member bracing system as shown in Fig. 1. If h and L are the height and width of a frame, respectively, the angle parameters are defined as: $0 < \beta < \tan^{-1}\frac{h}{L}$, $0 < \alpha < \tan^{-1}\frac{L}{h}$, $0 < \gamma_1 < 90°$, and $0 < \gamma_2 < 90°$. The share of each ODBS element from the lateral load is related to its orientation with

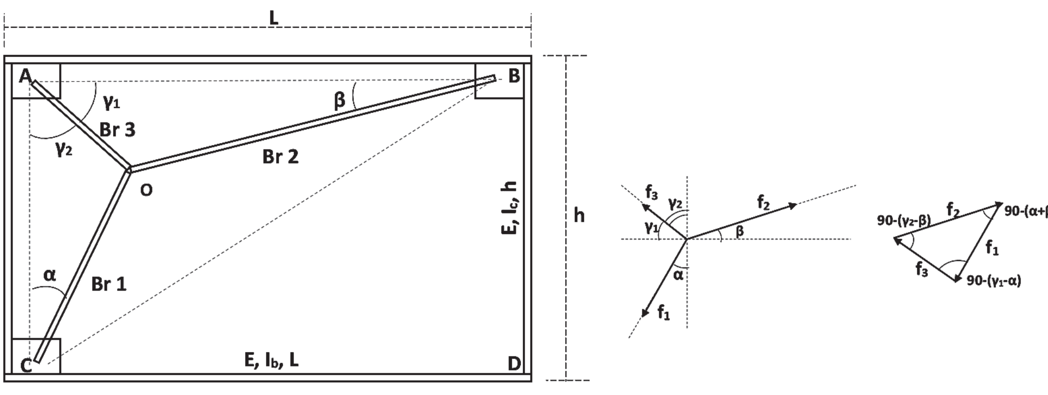

Fig. 1 *Parameter definitions and equilibrium conditions for an ODBS-braced RC frame*

respect to the direction of the diaphragm's inertial force. Under static horizontal loading, the share of the second member (Br-2 in Fig. 1) from the load is greater than its equivalent X and Inverted-V braces. This is because angle β is smaller than the angle of the diagonal, and Br-2 elements with smaller angles absorb a larger portion of a horizontally imposed load compared to elements with larger angles. The force of the Br-2 member is divided between the other two members, i.e., 1 and 3, through which it is transferred to the beam-column connections.

As observed in Fig. 1, there are many different locations for the placement of the members' intersection point O. If members 1 and 2 lie on the diagonal or near the diagonal, the angle between these two members and the third member is close to 90 degrees, which renders the third member ineffective. With reference to the force diagram of Fig. 1, the following equation holds true:

$$\frac{f_3}{\cos(\alpha+\beta)}=\frac{f_2}{\cos(\gamma_1-\alpha)}=\frac{f_1}{\cos(\gamma_2-\beta)} \quad (1)$$

If e denotes the off-diagonality of members 1 and 2, it can be expressed as e = OH´/AH, in which OH´ and AH are defined in Fig. 2. Now, as an example, for L/h = 1.5, if OH´/AH = 0.5 and by placing f_3 on a diagonal, then f_1 = 0.77, f_2 and f_3=1.02 f_1 and also for OH'/AH = 0.2, f_1=0.5 f_2 and f_3=0.3 f_2. Therefore, it seems that as e increases, the force in the third member (f_3) increases. On the other hand, as e decreases, the force in the second member (f_2) increases.

One of the characteristics of ODBS is that all the steel members fall either in tension or compression. Based on a linear analysis and assuming no axial deformations for the beams and columns, the state of equilibrium in the horizontal direction leads to Equation 2 as the shear resistance in the steel ODBS and RC frame according to the inter-storey lateral deformation.

$$\frac{\left\{\left(\frac{A_1E_1}{L_1}.\sin\alpha+\frac{A_3E_3}{L_3}.\cos\gamma_1\right).\frac{A_2E_2}{L_2}.\cos\beta\right\}}{\left\{\frac{A_1E_1}{L_1}.\sin\alpha+\frac{A_3E_3}{L_3}.\cos\gamma_1+\frac{A_2E_2}{L_2}.\cos\beta\right\}}+\frac{12EI_c}{h^3}\left[\frac{\frac{I_c}{h}+6\frac{I_b}{L_b}}{2\frac{I_c}{h}+3\frac{I_b}{L_b}}\right]=\frac{V_{i+1}-V_i}{\Delta_{i+1}-\Delta_i} \quad (2)$$

where E is Young's modulus for concrete, and E_1, E_2, and E_3 are, respectively, Young's modulus for steel brace members 1 to 3; I_b and I_c are, respectively, the beam and column moments of inertia, and L_b and h are the length of the beams and columns, respectively. Also, V_i and Δ_i denote storey shear and drift, respectively. The term of stiffness includes the sum of the lateral stiffness of the steel brace and moment frame. Since the moment frame remains elastic during lateral loading, the stiffness of MRF can readily be derived by the elastic analysis of the frame.

Equation 2 is considered for each ODBS-braced RC panel. The limits of V/Δ are related to the lateral stiffness of a single-span braced frame up to its yielding limit. For a more accurate model, the stiffness of gusset plates should also be considered as additional terms on the left-hand side of the equation. In general, for every model of steel-braced frame, the uncoupled Equation 3, expressed for storey and, governs.

$$[K_{\text{Steel Brace}}+K_{\text{MRF}}]_i=\frac{\partial V_i}{\partial \delta_i} \quad (3)$$

Based on an early investigation carried out by Bush and Jirsa [2], the best off-diagonality for an ODBS-braced RC frame is considered to be between 0.2 and 0.5 (Fig. 2). More recent investigations [19-21] have shown that the optimum area for placement of the members' intersection point, O, is the hatched region shown in Fig. 2.

The ODBS is a type of concentric bracing system; therefore, its members could be designed according to AISC (AISC, 1999). This off-diagonal steel brace system has high geometrical ductility when compared with an unbraced MRF system. As a result, under lateral

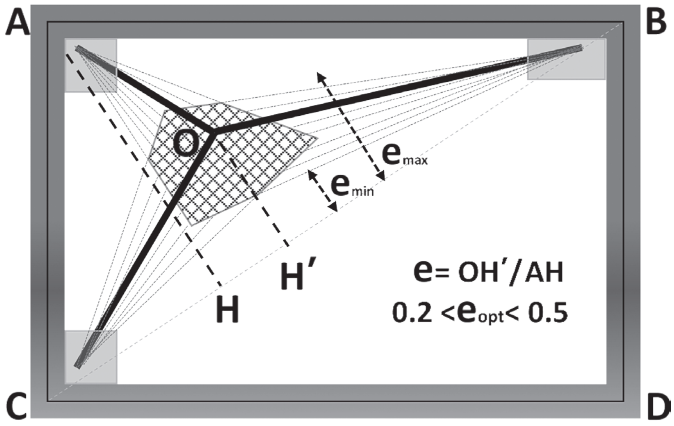

Fig. 2 *Optimum region for the intersection point O in ODBS*

loading, the ductility of the bracing system is utilized prior to that of the MRF, in effect saving the MRF's ductility capacity for higher loads. Another important point to be considered in design is that both steel bracing and MRF systems contribute to the shear resistance of a storey and should be separately considered. In an RC flexural frame, the columns are mainly responsible for resisting shear. Therefore, they should be designed according to a minimum 50% of the total lateral force. There are no reliable code provisions regarding the combined design of an RC flexural frame and steel brace. The load distribution can be divided into two parts, i.e., linear and nonlinear. Also, the material nonlinearity will affect lateral displacements. Therefore, at the start of the analysis, a linear load distribution is used to avoid any nonlinear parameter entering the analysis. As indicated in Fig. 1, the present parameters could be divided into two types, i.e., geometric and material properties. By considering the geometric characteristics of the members and the coordinates of the brace members' intersection point O, which is considered to be a pin connection, the members' forces could be established by equilibrium conditions.

3 RESPONSE OF AN ODBS BRACING SYSTEM TO CYCLIC LOADING

Since the capacity of a braced frame under cyclic loading depends on the capacity of the bracing system, the response of the bracing system alone to cyclic loading is first investigated. Several types of bracing systems are investigated to assess their energy dissipation capability and the performance of individual members under cyclic loading.

3.1 Response of a single member to cyclic loading

In this section, the cyclic response of a single brace member is investigated. When buckling occurs in a compressed member, the compression strength will be decreased due to a nonlinear plastic rotation in the mid-length of the axial member. According to the Baushinger effect and the in-plane and out-of-plane buckling occurring in previous cycles, the compressive strength is degraded during the subsequent cycles. This is a significant problem for members that are subjected to a dual tension/compression force. In the following, the response of the single brace member shown in Fig. 3 under the cyclic load protocol shown in the same figure is evaluated. The cyclic loading is applied in a displacement-controlled format, with an increasing axial deformation (normalized to L_B) every three cycles, as shown in Fig. 3.

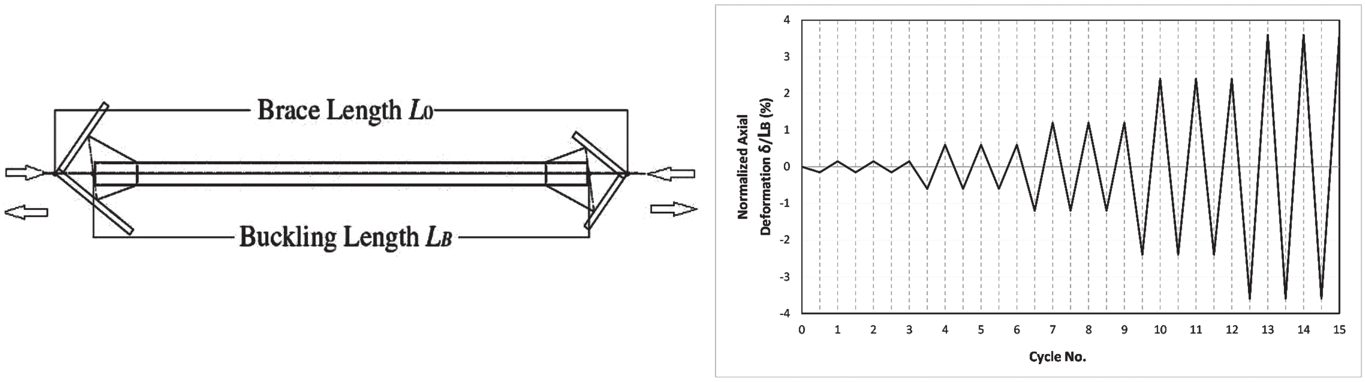

Fig. 3 *Bracing member and the cyclic loading protocol*

The material properties considered for steel are A500 Gr.B (ASTM A595, 2014). The dimensional properties of a single member are: the brace length, $l_0 = 4{,}2\,m$ buckling length, $l_B = 3.7\,m$, RHS 4 × 4 × 0.25 section with cross-sectional area, and $A_g = 23.16\ cm^2$. The ductility ratio is expressed as the ratio of the post-yield displacement to the yield displacement ($\mu = \delta_{max}/\delta_y$). Under this definition, the compressive strength of the bracing is in the form of μ multiples. The maximum compressive capacity at a member's first buckling may be expressed in terms of the member's elastic strength, i.e., A_gF_y . In this paper, the simplified expression given by Eq. 4 for a type of SSRC column (AISC, 1999) has been used to evaluate

$$C_u = \frac{A_g F_y}{(1+\lambda^{2n})^{1/n}} \tag{4}$$

Where λ is the column slenderness ratio, and n is the number related to the first buckling (n = 1.34) in accordance with AISC 1999 (AISC, 1999).

The cyclic response of a single member is shown in Fig. 4. In this figure, the force P and displacement δ are normalized to the yield capacity, P_y, and the yield displacement, δ_y. Also, the term C'_{un} signifies the compressive capacity corresponding to the ductility ratio, μ = n (n = 1, 2, etc.). The higher the value of the integer number n, the more ductility or post-buckling capacity the member will have. Usually the post-buckling starts at a compressive force of less than $0.5P_y$ and continues up to the member's failure. In Fig. 4, $\mu_F = \frac{(\delta^c_{max}+\delta^t_{max})}{\delta_y}$ is the total available ductility in both the tension and compression zones, and T_{max} is the maximum tensile resistance. The maximum required ductility (μ_{max}) in a symmetrical bracing system is about 3 to 4; however, this value may be increased to about 5 to 7 in special designs (O.F. Hassan et al., 1991; I.F. Khatib et al., 1988; A.M. Remennikov et al., 1998; ACI 318, 2005).

3.2 Ductility of ODBS compared to X bracing and Inverted-V bracing

One of the advantages of ODBS is the third member's shorter length compared to the brace members in X and Inverted-V bracing systems. Also, the resistance of concentric brace members under seismic loads depends on their buckling capacity due to load cycles and nonlinear deformations. In this section, a unit frame with hinged connections is considered to determine the response under the dynamic cyclic loading of three different types of bracing schemes, including X-brace, Inverted-V brace and ODBS. All the frame-brace systems were designed based on100% of the load being carried by the brace system. Due to the beam-column hinge connections considered for the RC frame, the RC members just behave as axial links and transfer the load between the brace members, except in Inverted-V bracing, in which the upper beam's flexural response contributes to the dissipation capacity of the frame-brace system. The unit frame's height (h) and length (L) are 3.5m and 5.5m, respectively. For the OBDS system, OH′/AH=0.2. Section U100 was selected for all the bracing members, and a single 12 mm thick plate was considered for all the gusset plates. The RC columns were 350 x 350 mm in the cross section and were reinforced by 12Ø18 longitudinal bars and a Ø8@150 mm transverse reinforcement. The beams were assumed to be 350 x 300 mm in the cross section and uniformly reinforced by 3Ø18 at the top and bottom with Ø8@150 mm as a transverse reinforcement. The same cyclic load protocol as given in Fig. 3 was applied to the three systems. The cyclic load was increased up to the maximum drift.

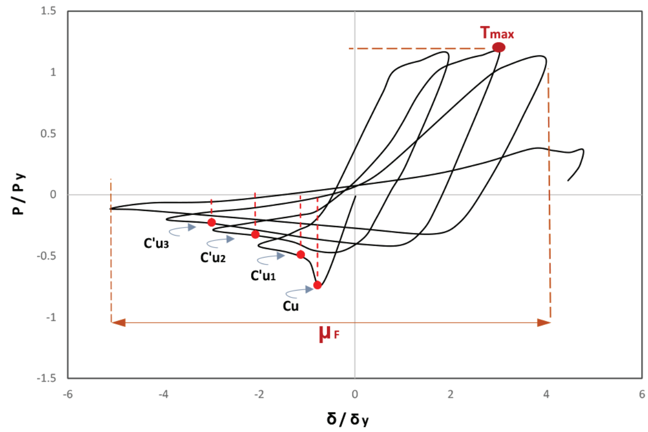

Fig. 4 *Hysteresis response of a brace member*

The hysteresis responses of the three bracing systems in the form of shear force versus lateral drift are compared in Fig. 5. As is observed in Fig. 5, the ODBS-braced frame has the highest amount of dissipated energy, E, in the bracing members, followed by the X-bracing system. Also, the primary and secondary compression capacities, and , are considerably higher in the ODBS compared to both the X and Inverted-V bracing systems.

4 COMPARATIVE STUDY OF BRACED MULTI-STOREY FRAMES

In this section, multi-storey RC frames retrofitted with different types of steel bracing systems, including X-brace, Inverted-V and ODBS systems, are subjected to different dynamic time history records and cyclic loading, so that the merits and shortcomings of each system can be evaluated and compared. Three 5-storey, 10-storey and

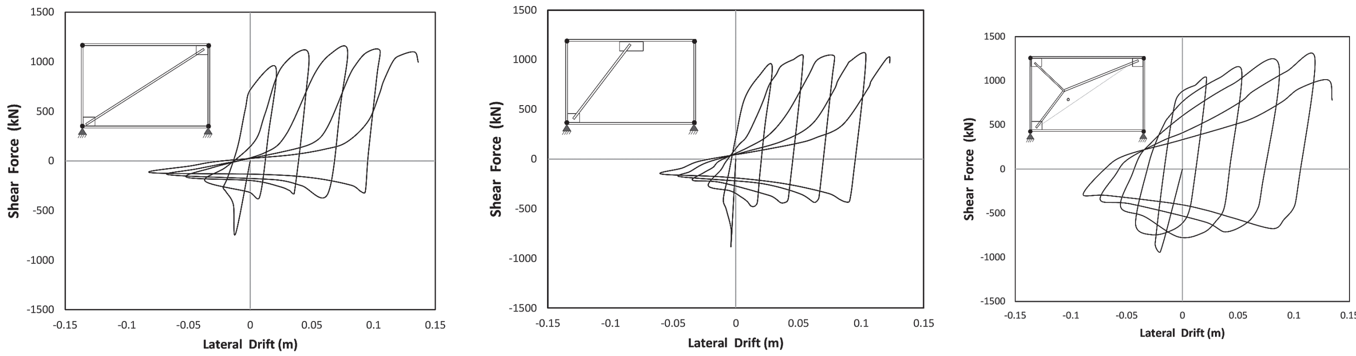

(a) (b) (c)

Fig. 5 *Hysteresis behaviour of bracing systems with asymmetric geometry during symmetric cyclic loading (drift); (a) X-braced, (b) inverted V-braced and (c) ODBS-braced frames*

15-storey 2D, RC frames were selected from a building with a rectangular plan of 20 m by 15 m in longitudinal and transverse directions, respectively. The selected 2D frames are in a transverse direction; they comprise three 5.0 m long bays.

4.1 Geometry and design of the frames

The geometry of the selected frames (5, 10 and 15 stories) with four bracing conditions (MRF, X, Inverted-V and ODBS) are shown in Fig. 6. The diaphragms are assumed to be rigid; they transfer a distributed dead load and a live load of 4.6 kN/m^2 and 2.0 kN/m^2, respectively. All the beam-column connections, as well as the column-foundation connections, are also assumed to be rigid.

Since ductility is a major performance parameter for a seismic response, the principal design criterion is based on the maximum allowable drift, δ_{max}. The frames were designed based on a ductile design of dual systems in accordance with ACI-318 provisions for MRF intermediate ductility (ACI 318, 2005). The design parameters selected for the three types of frames are listed in Table 1.

Tab. 1 *Design criteria and parameters for the steel-braced RC frame models*

Parameter	5 storey	10 storey	15 storey
Drift Limit, θ_d	0.025	0.025	0.025
Effective mass, m_e (kN)	2908	5821	8728
Effective height, H_e (mm)	12.843	24.424	36.045
Design displacement, Δ_d (mm)	306	550	780
Equivalent damping, ζ_{eq}	13.6	13.7	13.5
Effective period, T (s)	2.125	3.312	4.130
Base shear (kN)	814	1240	1623

STAAD-Pro V8i software (3D Structural Analysis and Design Software, 2012) was utilized to carry out the necessary analysis and design. The concrete and steel were modeled using solid elements with material properties as shown in Fig. 7. The characteristics of the RC elements, which were designed on the above basis, are listed in Table 2. Also, Ø10 shear reinforcements were used at 100 mm and 200 mm spacing for the inner and outer areas of the critical shear zones, respectively.

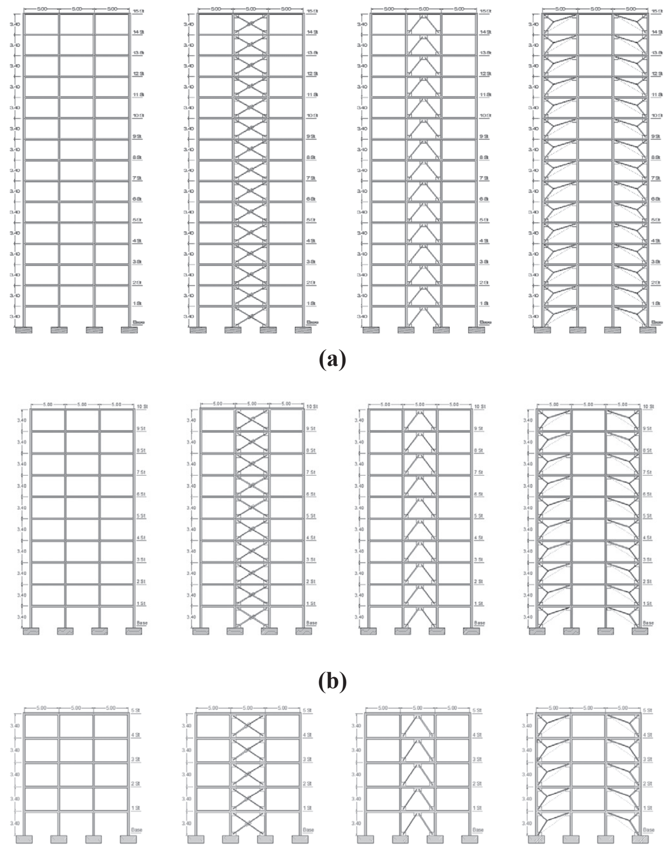

Fig. 6 *Geometry and bracing configurations of a (a) 15-storey frame, (b) 10-storey frame and (c) 5-storey frame*

For each type of bracing system, the steel sections and gusset plates were designed based on the provisions of AISC-05 (SAP2000, 2015). The 2U-Section was selected for all the brace elements. Table 3 shows the size of the brace and gusset elements in each type of bracing system and frame number of storeys.

For each type of bracing system, the steel sections and gusset plates were designed based on the provisions of AISC-05 (SAP2000, 2015). The 2U-Section was selected for all the brace elements. Table 3 shows

Tab. 2 *Intermediate MRF RC members' characteristics*

Storey No.	Column Sections (Square, cm)			Beam Sections (BxH, cm)		
	5-Storey Frame	10-Storey Frame	15-Storey Frame	5-Storey Frame	10-Storey Frame	15-Storey Frame
1	□ 40x40 – 12Ø20	□ 60x60 – 24Ø20	□ 80x80 – 32Ø20	□ 40x35 – top: 4Ø20 Bot: 4Ø20	□ 60x50 – top: 7Ø20 Bot: 7Ø20	□ 80x70 – top: 9Ø20 Bot: 9Ø20
2	□ 40x40 - 12Ø20	□ 60x60 – 24Ø20	□ 80x80 – 32Ø20	□ 40x35 – top: 4Ø20 Bot: 4Ø20	□ 60x50 – top: 7Ø20 Bot: 7Ø20	□ 80x70 – top: 9Ø20 Bot: 9Ø20
3	□ 35x35 – 8Ø20	□ 50x50 – 20Ø20	□ 70x70 – 28Ø20	□ 35x30 – top: 3Ø20 Bot: 3Ø20	□ 50x45 – top: 6Ø20 Bot: 6Ø20	□ 70x60 – top: 8Ø20 Bot: 8Ø20
4	□ 35x35 – 8Ø20	□ 50x50 – 20Ø20	□ 70x70 – 28Ø20	□ 35x30 - top: 3Ø20 Bot: 3Ø20	□ 50x45 – top: 6Ø20 Bot: 6Ø20	□ 70x60 – top: 8Ø20 Bot: 8Ø20
5	□ 30x30 – 8Ø20	□ 45x45 – 16Ø20	□ 60x60 – 24Ø20	□ 30x30 – top: 3Ø20 Bot: 3Ø20	□ 45x40 – top: 5Ø20 Bot: 5Ø20	□ 60x50 – top: 7Ø20 Bot: 7Ø20
6	-	□ 45x45 – 16Ø20	□ 60x60 – 24Ø20	-	□ 45x40 – top: 5Ø20 Bot: 5Ø20	□ 60x50 – top: 7Ø20 Bot: 7Ø20
7	-	□ 40x40 – 12Ø20	□ 50x50 – 20Ø20	-	□ 40x35 – top: 4Ø20 Bot: 4Ø20	□ 50x45 - top: 6Ø20 Bot: 6Ø20
8	-	□ 40x40 - 12Ø20	□ 50x50 – 20Ø20	-	□ 40x35 – top: 4Ø20 Bot: 4Ø20	□ 50x45 – top: 6Ø20 Bot: 6Ø20
9	-	□ 35x35 - 8Ø20	□ 45x45 - 16Ø20	-	□ 35x30 – top: 3Ø20 Bot: 3Ø20	□ 45x40 – top: 5Ø20 Bot: 5Ø20
10	-	□ 30x30 – 8Ø20	□ 45x45 – 16Ø20	-	□ 30x30 – top: 3Ø20 Bot: 3Ø20	□ 45x40 – top: 5Ø20 Bot: 5Ø20
11	-	-	□ 40x40 - 12Ø20	-	-	□ 40x35 – top: 4Ø20 Bot: 4Ø20
12	-	-	□ 40x40 - 12Ø20	-	-	□ 40x35 – top: 4Ø20 Bot: 4Ø20
13	-	-	□ 35x35 – 8Ø20	-	-	□ 35x30 – top: 3Ø20 Bot: 3Ø20
14	-	-	□ 35x35 – 8Ø20	-	-	□ 35x30 – top: 3Ø20 Bot: 3Ø20
15	-	-	□ 30x30 – 8Ø20	-	-	□ 30x30 – top: 3Ø20 Bot: 3Ø20

the size of the brace and gusset elements in each type of bracing system and frame number of storeys.

Different brace members have different slenderness ratios due to their different lengths and sizes. Table 4 indicates the slenderness ratio values for each type of bracing element. The slenderness ratios are presented for both the in-plane and out-of-plane directions as the main directions of the rectangular section.

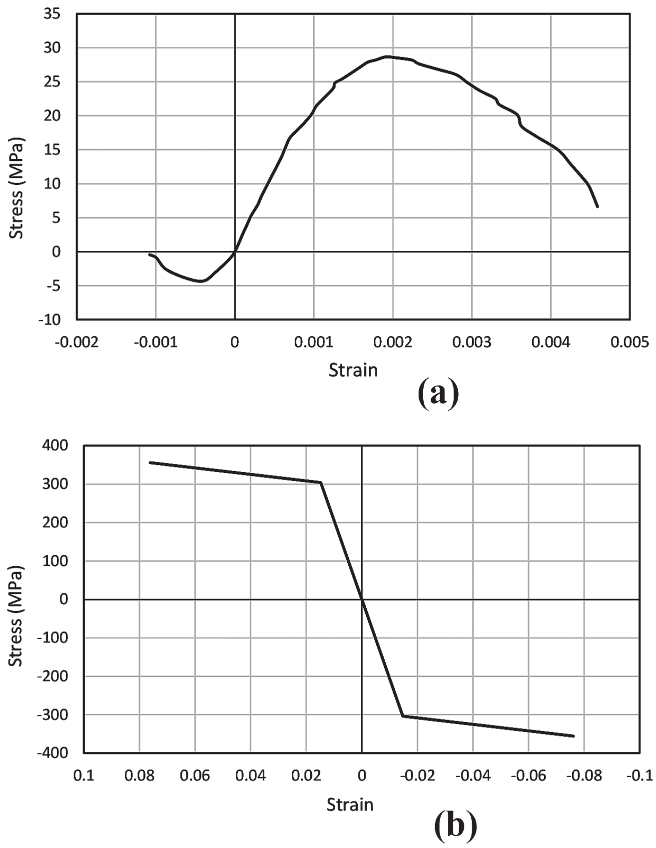

Fig. 7 *Material characteristics of: (a) concrete and (b) steel*

4.2 Dynamic properties of the selected frames

Prior to the time history and cyclic response analyses of the selected frames, modal analyses were conducted to evaluate the natural periods of the vibration of the frame-brace systems and the modal participation of the main modes of vibration. The values of these parameters for the first three lateral modes of the 12 brace-frame configurations are listed in Table 5. As can be seen in Table 5, the ODBS retrofitted frames exhibit a much more flexible response with the fundamental modes of vibration having higher periods of vibration and a lower mass participation factor. This shows that the number of effective modes participating in the response of frames retrofitted with ODBS is higher than that in the other systems.

4.3 Seismic excitation

Two sets of earthquake records were used as seismic excitation for the frames under investigation. The first set, which is listed in Table 6, includes the Kobe, Northridge, San Fernando, and El Centro earthquake records. They were selected according to their range of strong frequency contents; only the first 20 seconds of the records are considered. The second set (Table 6) includes the Tabas, Naghan and again the El Centro earthquake records. The amplitudes of these records were normalized to a PGA of 0.3g. The time histories of the first set of records are shown in Fig. 8 and those of the second set are shown in Fig. 9. The two sets of selected and scaled records cover a wide range of earthquake inputs for the different braced and unbraced frames under consideration.

Tab. 3 *Designed sections for steel brace members and gusset plates*

Types	Storey		Cross Section	Gusset Plates (mm)
Inverted V Brace	1, 2, 3, 4		2U 120	Single plate 20
	5, 6[1] ,7 ,8		2U 100 +2PL 80x8	Single plate 20
	9, 10, 11[2], 12		2U 100	Single plate 15
	13, 14, 15		2U 100	Single plate 15
X Brace	1, 2, 3, 4		2U 100 +2PL 80x8	Single plate 20
	5, 6[1], 7, 8		2U 120	Single plate 20
	9, 10, 11[2]		2U 100	Single plate 15
	12, 13, 14, 15		2U 80	Single plate 15
ODBS	**1st & 2nd members**	1, 2, 3, 4	2U 100 +2PL 80x8	Single plate 15
		5, 6[1], 7	2U 120	Single plate 15
		8, 9, 10, 11[2]	2U 120 +2PL 80x8	Single plate 15
		12, 13, 14, 15	2U 100	Single plate 15
	3rd member	1, 2, 3, 4	Tube 70x70x5	Double plate 12
		5, 6[1], 7	Tube 70x70x5	Double plate 12
		8, 9, 10, 11[2]	Tube 70x70x5	Double plate 12
		12, 13, 14, 15	Tube 50x50x4	Double plate 10

[1] For the 10-story specimens, steel bracing sections were selected from 6 to 15 of this table instead of 1 to 10.
[2] For the 5-story specimens, steel bracing sections were selected from 11 to 15 of this table instead of 1 to 5.

Tab. 4 *Slenderness ratio (kl/r) for different steel bracing elements*

Model	Types of brace	Cross Sections (cm)	In-Plane Buckling	Out-of-Plane Buckling
Off-Diagonal Brace	BR1	2U12+2PL8x0.8	58	55.4
		2U10+2PL8x0.8	66.7	61.9
		2U12	71.1	76.8
		2U10	85	96.2
	BR2	2U12+2PL8x0.8	39.2	37
		2U10+2PL8x0.8	45.1	43
		2U12	48	56.3
		2U10	57.6	64.4
	BR3	Tube 7x7x0.5	60.7	58.8
		Tube 5x5x0.4	85.9	81.5
Inverted-V Brace	BR1[1]	2U10+2PL8x0.8	82.3	70.7
		2U12	87.3	83.8
		2U10	104.7	96.54
X Brace	BR1[1]	2U10+2PL8x0.8	118.5	102.6
		2U12	126	116.9
		2U10	151.1	142.4
		2U8	186.2	169.8

[1] The same section is used for all members of the bracing system

Tab. 5 *Dynamic properties of selected models*

Frame Type	No. of Stories	1st Mode		2nd Mode		3rd Mode	
		Period T_1	**Mass Participation Factor**	**Period T_2**	**Mass Participation Factor**	**Period T_3**	Mass Participation Factor
MRF	5	1.21	0.66	1.03	0.21	0.61	0.06
Inverted-V	5	1.11	0.72	0.91	0.20	0.47	0.04
X-Braced	5	0.51	0.81	0.37	0.14	0.22	0.03
ODBS	5	1.17	0.51	1.19	0.32	0.94	0.14
MRF	10	2.08	0.58	1.83	0.28	1.24	0.09
Inverted-V	10	1.91	0.64	1.65	0.24	1.16	0.07
X-Braced	10	1.13	0.71	0.96	0.21	0.45	0.06
ODBS	10	2.31	0.48	2.45	0.41	1.38	0.12
MRF	15	3.02	0.59	1.96	0.29	1.63	0.09
Inverted-V	15	2.71	0.65	2.62	0.21	2.06	0.12
X-Braced	15	1.69	0.69	1.32	0.20	1.12	0.07
ODBS	15	3.66	0.43	3.78	0.31	2.85	0.15

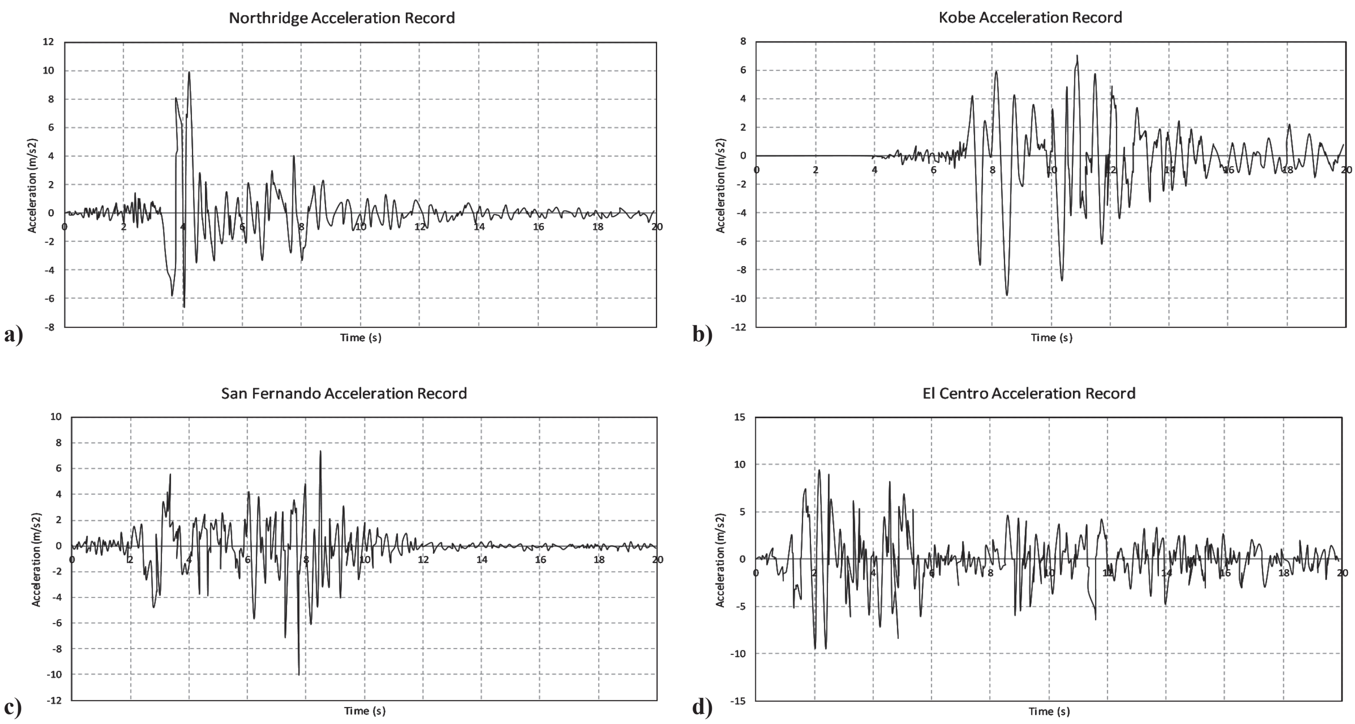

Fig. 8 *Ground acceleration time histories of the (a) Northridge, (b) Kobe, (c) San Fernando and (d) El Centro earthquakes (the first 20 seconds)*

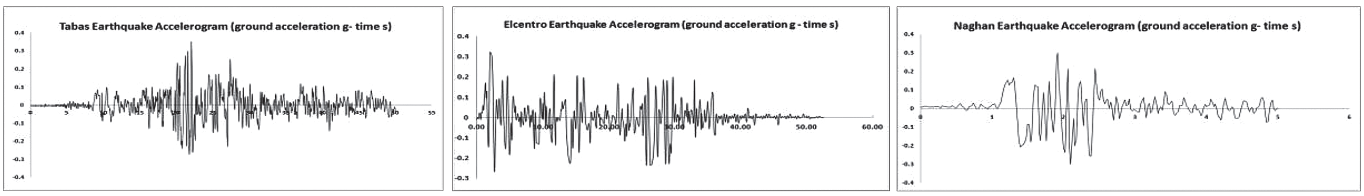

(a) **(b)** **(c)**

Fig. 9 *Ground acceleration time histories of the (a) Tabas, (b) El Centro and (c) Naghan earthquakes, all normalized to a PGA of 0.3g*

Tab. 6 *Properties of the earthquake accelerograms considered*

Records	Considered Duration (s) (max range)	PGA m/sec2 (g)	Time Step (s)	Type	Date of Event	Station	Comp.	Criterion for use in this research
Kobe	20 (7.5-12.5)	0.616	0.01	near field	1995	Takatori	Tak90	Frequency range: 0.3-1.10 Hz
Northridge	20 (3.5-8.0)	0.883	0.02	near field	1994	Santa Monica	N90E	Frequency range: 0.14-1.07 Hz
San Fernando	20 (4.5-9.5)	1.075 (rock)	0.01	far field	1971	Pacomia Dam	S74W	Frequency range: 0.6-4.40 Hz
El Centro	20 (1.5-5.5)	0.32 (stiff)	0.01	far field	1940	117 Array#9	EL-180	Frequency range: 0.4-6.40 Hz
Tabas	50	0.93	0.02	far field	1978	N16W	DAY-TR	PGA scaled to 0.3g
Naghan	5	0.72	0.005	near field	1977	LNG-09	N00E	PGA scaled to 0.3g
El Centro	53.7	0.32	0.01	far field	1940	117 Array#6	EL-180	PGA scaled to 0.3g

4.4 Time history response of a 10-storey RC frame with different bracing systems

In order to evaluate the acceleration and displacement responses of various X, Inverted-V, and ODBS bracing systems, a mid-rise, 10-storey frame was selected. The three frame-brace systems were subjected to the first set of selected accelerograms. The roof acceleration and displacement responses of the three braced systems to the time history records of the Northridge, Kobe, San Fernando and El Centro earthquakes are shown in Figs. 10 to 13, respectively. These figures indicate that in all four earthquakes, the acceleration response of the ODBS was markedly lower than those of the other two bracing systems; it was followed by the Inverted-V bracing system, with the X-braced system showing the highest acceleration response. This shows a much reduced base shear in the case of ODBS and therefore a more advantageous response. As for the acceleration response of the ODBS system in various earthquakes with different frequency contents, Figs. 10 to 13 show that this system has performed best according to records containing higher frequency ranges (such as the El Centro record). As the strong frequency range of a record decreases, the efficiency of the ODBS somewhat lessens, but always maintains its superior performance compared to the other bracing systems. Regarding the displacement response of the braced frames, the three bracing systems appear to behave differently in different earthquakes, so that a definitive conclusion cannot be made. Compared to the other systems, the ODBS shows a relatively larger displacement response at first but invariably shows a reduced response in the latter parts of a record.

4.5 Time history hysteresis response of frames with different bracing systems

In order to assess the energy dissipation capacities of the three bracing systems, a second set of earthquake records, including those

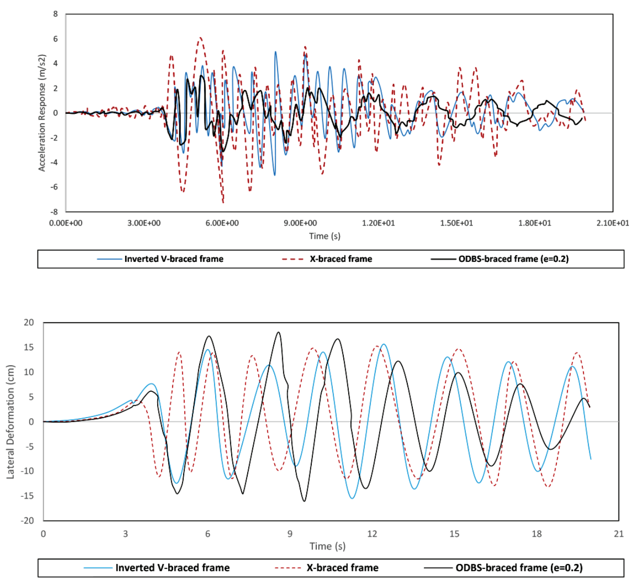

a)
b)

Fig. 10 *(a): Acceleration responses and (b): displacement responses of the 10-storey braced frames under the Northridge earthquake record*

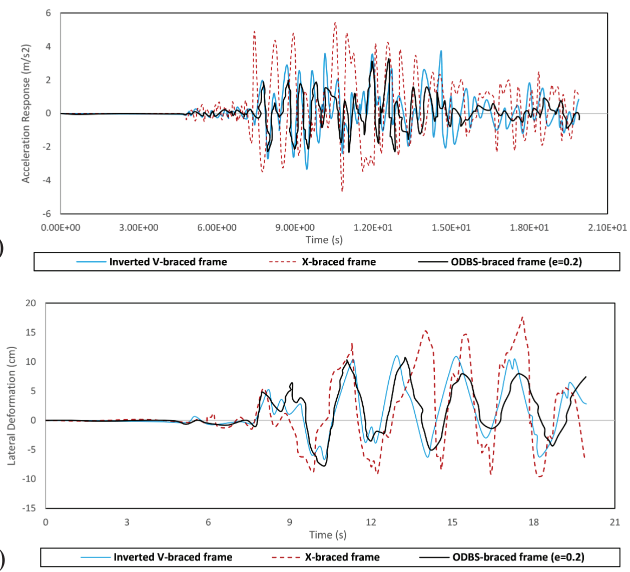

a)
b)

Fig. 11 *(a): Acceleration responses, and (b): displacement responses of the 10-storey braced frames under the Kobe earthquake record*

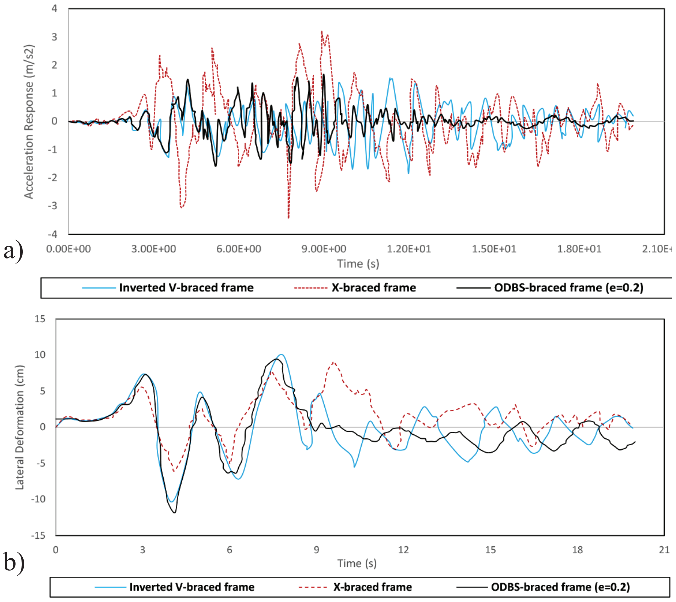

Fig. 12 *(a): Acceleration responses, and (b): displacement responses of the 10-storey braced frames under the San Fernando earthquake record*

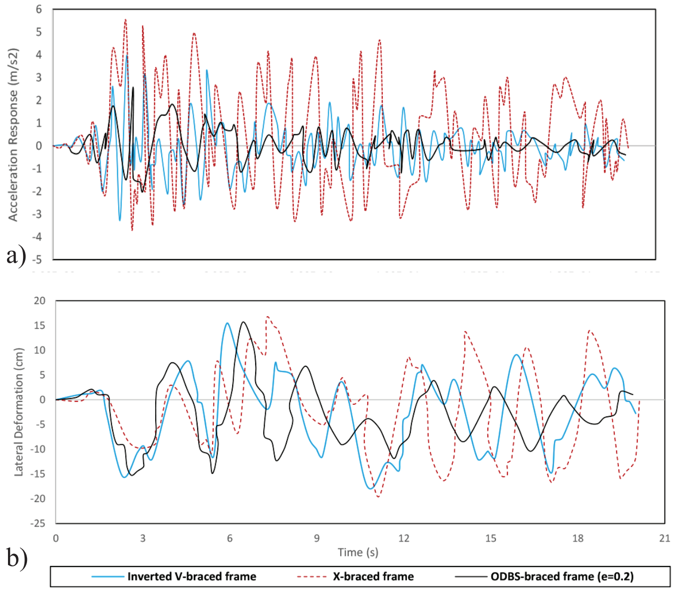

Fig. 13 *(a): Acceleration response, and (b): displacement response of the 10-storey braced frames under the El Centro earthquake record*

for the Tabas, El Centro and Naghan earthquakes was selected. To have a sound basis for comparison, these records were all normalized to a PGA of 0.3 g (Fig. 9). A response hysteresis curve is an important property for assessing the performance of structures under dynamic loading. In these analyses, the base shear variation with the time during each record was evaluated and plotted against the top floor displacement. The time history hysteresis diagrams for the 10-storey frame model retrofitted with three bracing systems were compared with each other and that of the non-retrofitted MRF in Fig. 14 for the response under the El Centro earthquake record, in Fig. 15 for the response under the Naghan earthquake record, and in Fig. 16 for the response under the Tabas earthquake record.

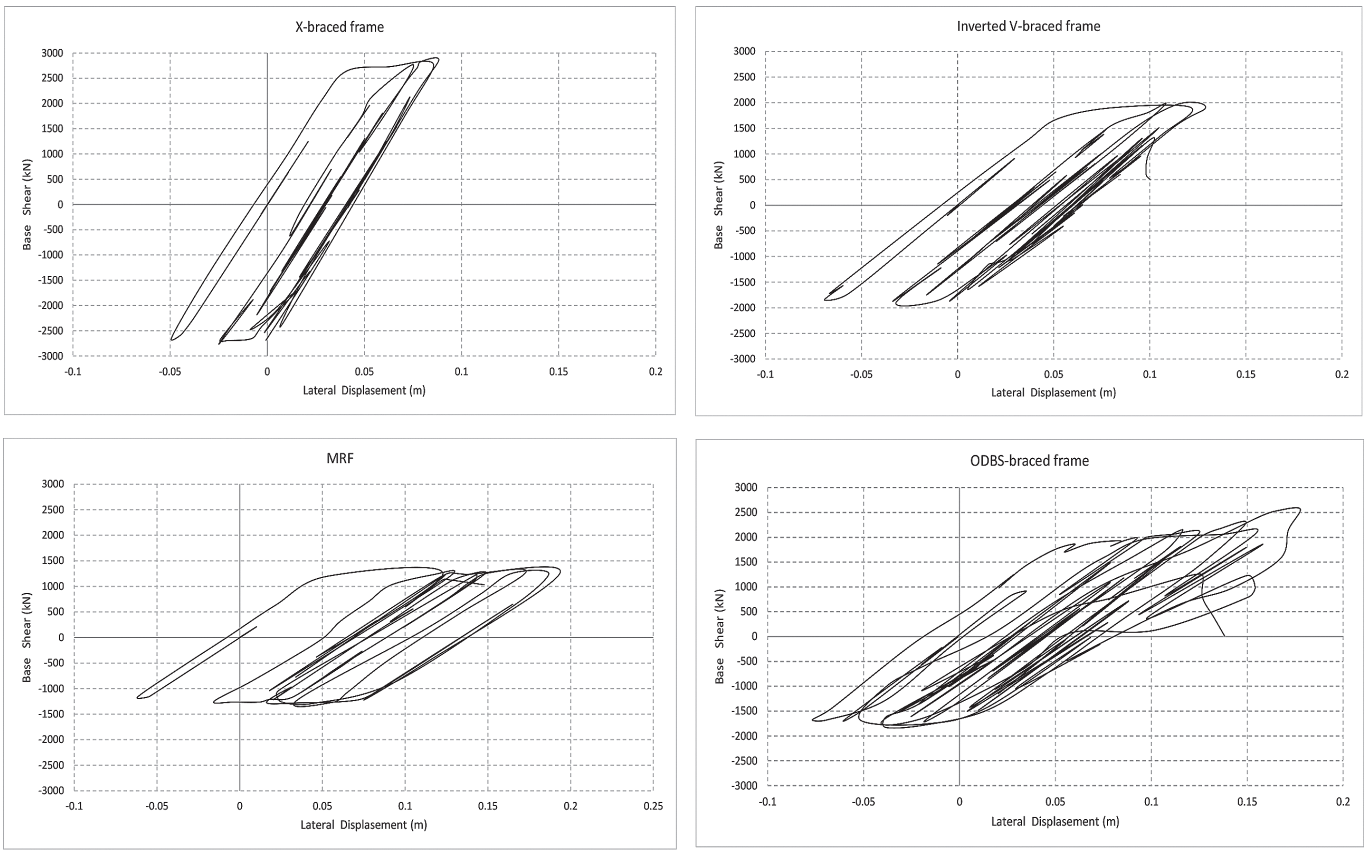

Fig. 14 *Time history hysteresis response of the 10-storey RC frame with different retrofitting configurations under the scaled El Centro accelerogram*

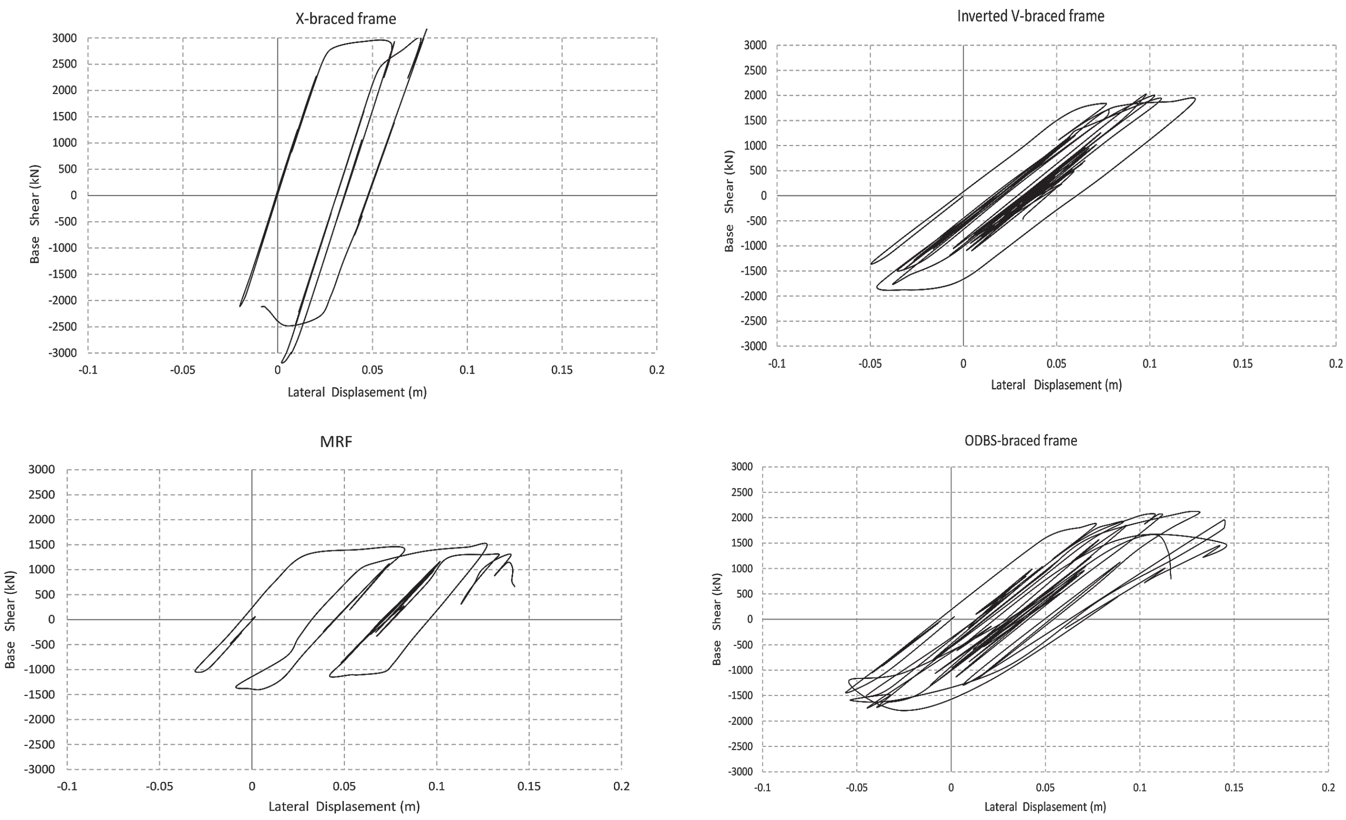

Fig. 15 *Time history hysteresis response of the 10-storey RC frame with different retrofitting configurations under the scaled Naghan accelerogram*

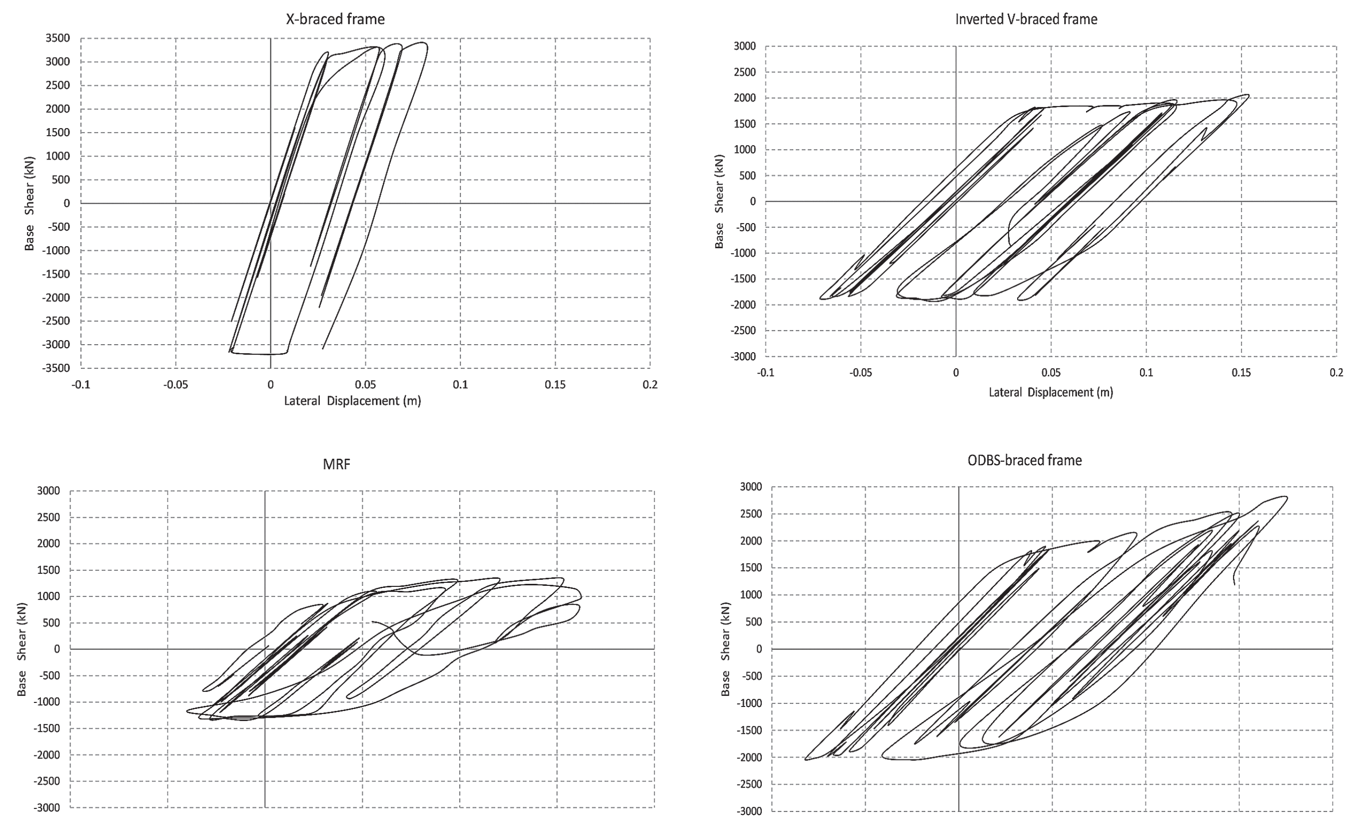

Fig. 16 *Time history hysteresis response of the 10-storey RC frame with different retrofitting configurations under the scaled Tabas accelerogram*

Figs. 14 to 16 show that the RC frames in all four retrofitting configurations behaved in an approximately elastic manner in the first cycle. The stiffness of the MRF, Inverted-V and X-braced models gradually degrade in subsequent cycles, but the RC frame with ODBS does not degrade in several cycles. With the ODBS RC frame, the plastic deformation increases, and the hysteresis loops become wider, which reflect the high capacity of energy dissipation for this system. The X-braced frame has little plastic deformation under this loading protocol. Considering the high stiffness of the X-braced system, the rigidity in subsequent cycles is the same as in the first one. Based on the results obtained, it is evident that the X-braced RC frame exhibits the highest strength capacity and the lowest energy absorption capacity in comparison with the other systems. After the X-braced system, the Inverted V-braced RC frame had the highest capacity with an increased amount of ductility, when compared to the X-braced frame. On the other hand, the ODBS hysteresis curves show the highest amount of energy dissipation, but with an expectedly reduced capacity. The results of the time history hysteresis response indicate that most of the buckling in the ODBS occurred in a deformation range from $2\Delta_y$ to $4\Delta_y$, which is a much larger deformation range in comparison with the other bracing systems.

4.6 Response to cyclic loading

The cyclic response investigation of the multi-storey frames was conducted in two parts. First, the effect of the number of stories on the response of the RC frame retrofitted with ODBS was explored; secondly, the cyclic responses of the 15-storey frame with different retrofitting configurations were evaluated.

Fig. 17 shows the cyclic load protocol used in the first part of the investigation of 5, 10 and 15-storey frames retrofitted with ODBS. The loading of the frames was force controlled. Lateral loads were applied with increasing magnitudes in each cycle, and the displacement was measured at the end of each cycle. The hysteresis loops obtained from the cyclic loading for the ODBS models with different numbers of stories are plotted in Fig. 18.

Fig. 18 shows that all the RC frames retrofitted with ODBS dissi-

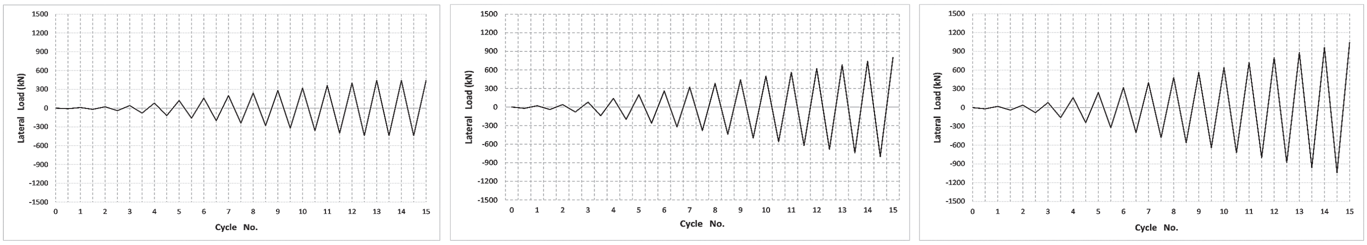

a) b) c)

Fig. 17 *Cyclic load protocols used for: (a) 5-storey, (b) 10-storey and (c) 15-storey ODBS retrofitted frames*

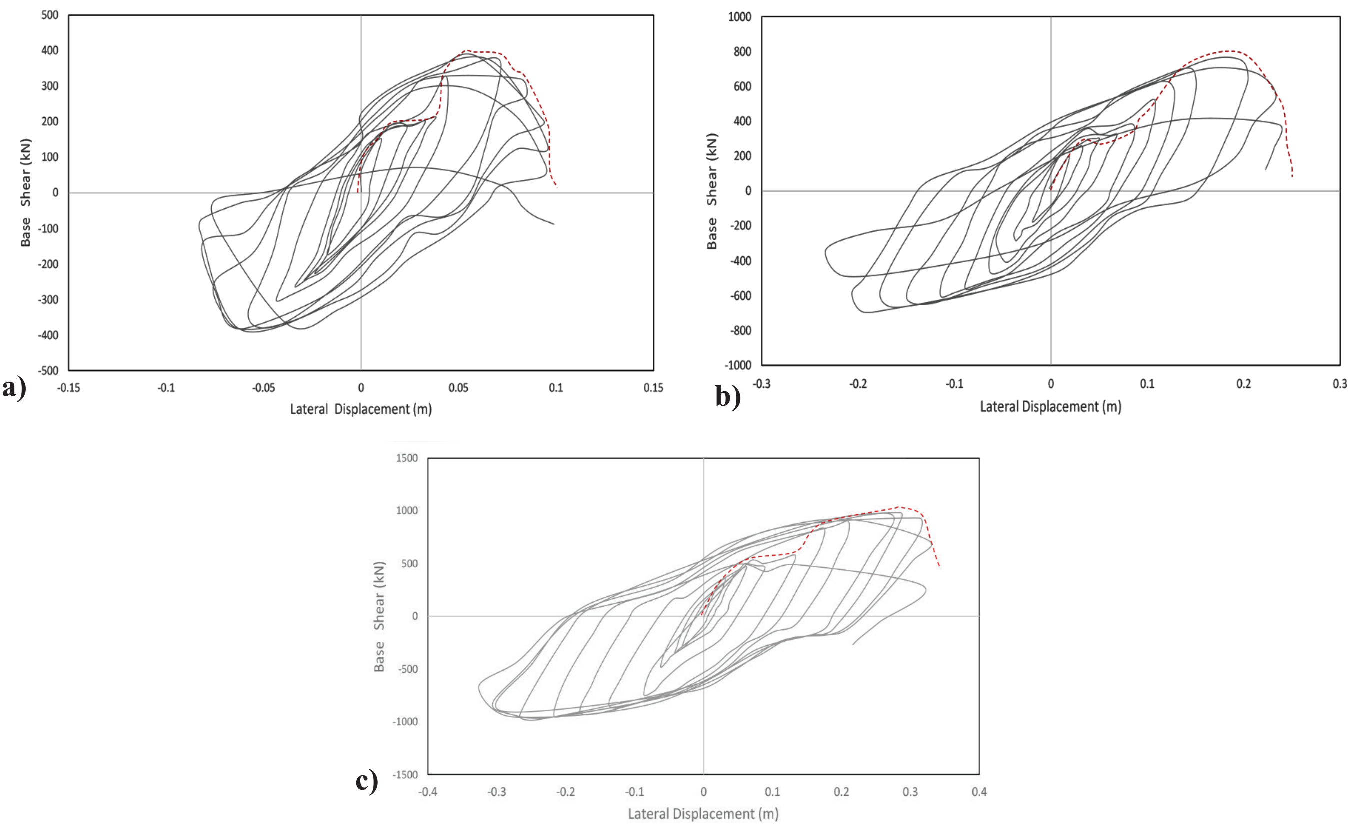

Fig. 18 *Load-displacement cyclic response of: (a) 5-storey, (b) 10-storey and (c) 15-storey ODBS retrofitted frames*

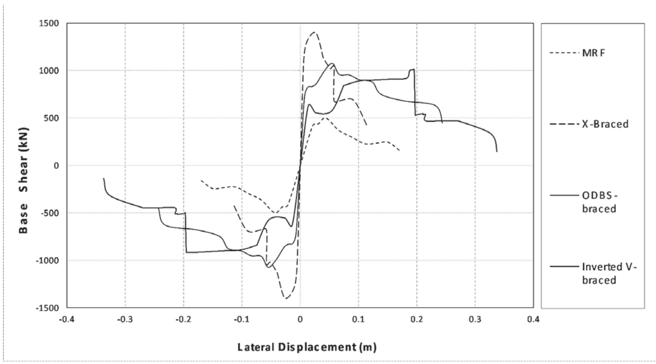

Fig. 19 *Comparison of the back-bone curves of the 15-storey frame with different retrofitting configurations*

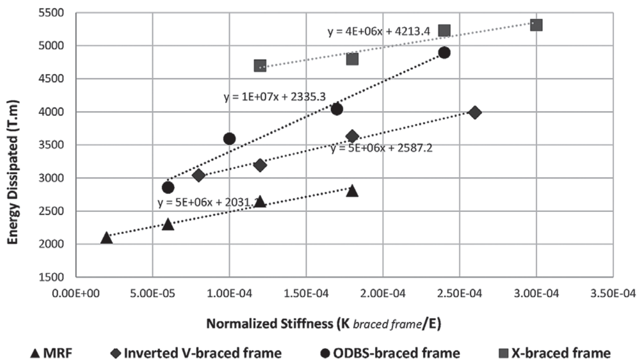

Fig. 20 *The relationship between the energy dissipated and lateral stiffness of unit RC frames with different retrofitting configurations*

pate large amounts of energy during the latter loading cycles. It also indicates that the ODBS dissipates more energy in the frames with a smaller number of stories, which indicates that it is more effective in low-rise buildings. A back-bone curve can be obtained by connecting the peak points of the hysteresis curve in every level of the loading. A back-bone curve is used to observe the deformation capacity and strength decay of the specimens [20]. It is similar to the force-displacement capacity curve obtained from a non-linear static pushover analysis and contains large amounts of information regarding the lateral-resisting properties of sway frames. The back-bone curves for the three ODBS retrofitted frames were also plotted in the respective hysteresis response in Fig. 18.

In the second phase of the cyclic loading investigation, the 15-storey frames with different retrofitting configurations were selected and subjected to the cyclic loading protocol shown in Fig. 17-c. The hysteresis loops for the four models were evaluated, and the back-bone curves of the hysteresis responses were extracted. The back-bone curves for the four retrofitting configurations of the 15-storey RC frame are compared in Fig. 19. With reference to Fig. 19, it is evident that the non-retrofitted MRF exhibits the least amount of energy absorption capacity. The X-bracing system is the stiffest and provides the highest resistance, but the ODBS system has the largest area under the force-displacement curve and provides the greatest energy dissipation capacity.

4.7 Energy dissipation versus the retrofitted frame stiffness

The amount of energy dissipation is not only a function of the ductility of a system, but also its stiffness. To gain a better understanding of the relationship between energy dissipation and stiffness in different retrofitting schemes, a one-span, one-storey unit RC frame was considered and subjected to cyclic loading based on the protocol shown in Fig. 3. The relations between the energy dissipated and the RC frame's stiffness in the four retrofitting configurations are plotted in Fig. 20. The stiffness of the frames is shown on the horizontal axis as normalized to the steel elastic modulus E. A linear relation is extracted from the results for all four retrofitting configurations as shown in Fig. 20. It can be noted that the slopes of the trend lines have a direct relation with the amount of energy dissipated. The slope of the energy dissipation-stiffness line for ODBS is markedly higher than the other three configurations, which indicates that the rate of increase in energy dissipation with increasing stiffness is greater in the ODBS compared to the other retrofitting configurations.

4.8 Out-of-plane buckling of ODBS at a conjunction joint

As indicated in Fig. 21, the global out-of-plane buckling of an ODBS system at the intersection point of a brace should be avoided since this type of failure drastically reduces the strength of the bracing system. One method to increase the out-of-plane stiffness of the bracing system and avoid this global buckling is to use a double-plated connection intersection for the point so that the out-of-plane rotation of the bracing members can be controlled. However, as the intersection point should act as a hinge, the connection should be designed in such a way as to allow for the in-plane rotation of the brace members. A proposed double-plated central connection is shown in Fig. 22.

In this section, the cyclic response of a 5-storey RC frame retrofitted with ODBS is evaluated under two different, i.e., (i) single plate and (ii) double plate, configurations for the intersection connection point. The ODBS arrangement in the frame and details of the connections are shown in Fig. 23. The material properties considered for the concrete and steel are the same as those given in Fig. 7. The frame-brace assemblage was subjected to the cyclic loading protocol shown in Fig. 24.

The hysteresis of a storey load versus storey drift in a typical storey for single-plated and double-plated configurations is plotted in Fig. 25. With reference to Fig. 25, it is clear that the double-plated central connection has resulted not only in a 25% increase in the capacity of the frame-bracing system, but also in wider hysteresis loops that signify a substantial increase in the energy absorption capacity of the system. The pinching in the hysteresis loops and reduced capacity of the single-plated connection is evidently due to the out-of-plane buckling of this type of central connection.

To further evaluate the responses of the two central connection types, the stiffness and dissipated energy of the ODBS with the two types of connections in all the loading cycles are plotted in Figs. 26 and 27, respectively. Fig. 26 indicates a larger degree of stiffness and a steeper degradation for the double-plated connection up to loading cycle 6, after which the two connection types exhibit a somewhat similar response. Also, Fig. 27 shows that in the ODBS with the double-plated central connection, a substantially larger amount of energy is dissipated in different loading cycles compared to the single-plated case.

5 CONCLUSIONS

A number of full scale 2D numerical models, with low to mid-rise moment-resisting RC frames, were retrofitted with different types of bracing systems, including ODBS, Inverted-V, and X-Brace and sub-

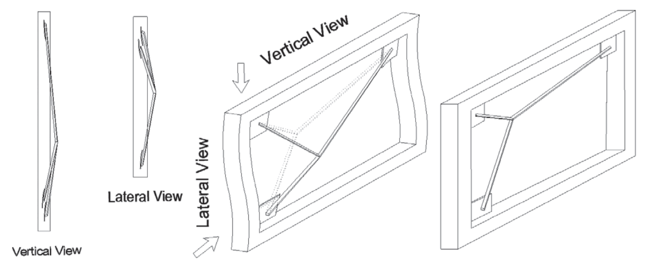

Fig. 21 *Perspective and 2D views of out-of-plane buckling of ODBS*

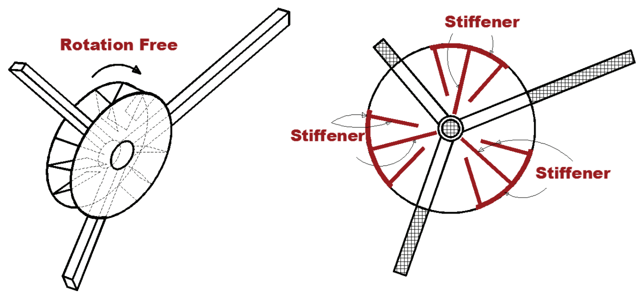

Fig. 22 *Details of a proposed double-plated ODBS intersection connection*

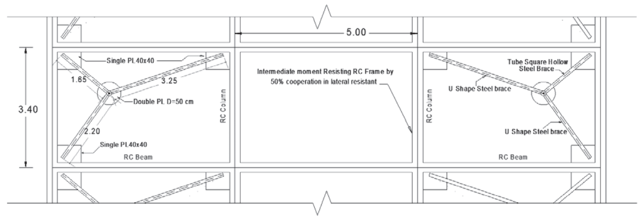

Fig. 23 *Geometry and details of an ODBS-retrofitted-RC frame in a double plate configuration for a central connection (all dimensions in m)*

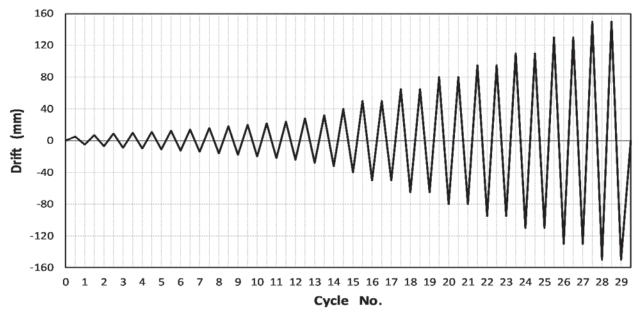

Fig. 24 *Cyclic loading characteristics for the out-of-plane buckling investigation*

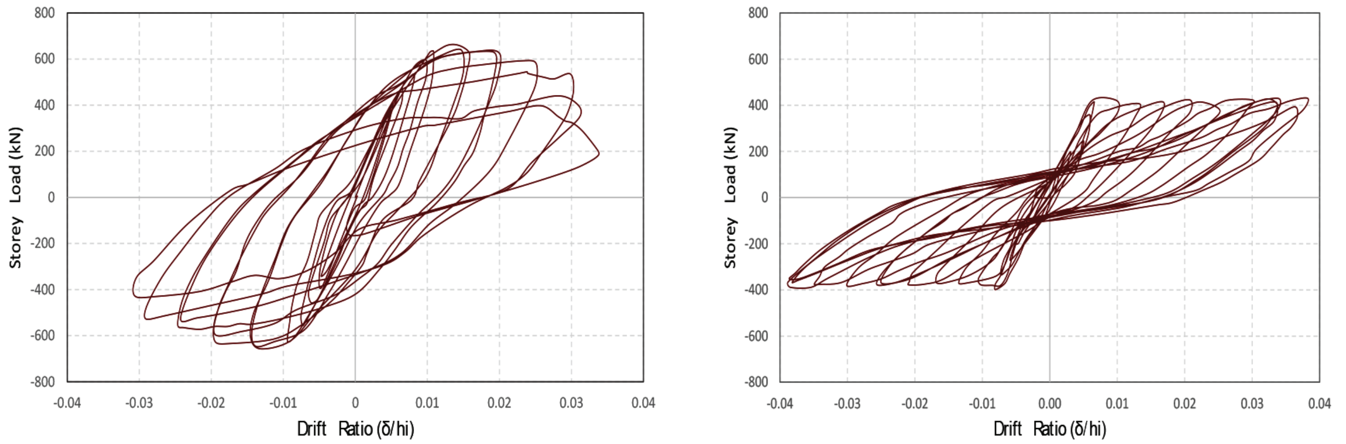

Fig. 25 *Hysteresis response of ODBS with (a) double and (b) single-plated central connections*

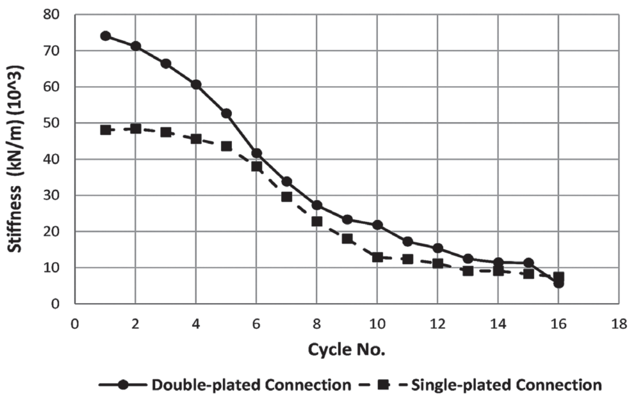

Fig. 26 *Degradation of stiffness during cyclic loading*

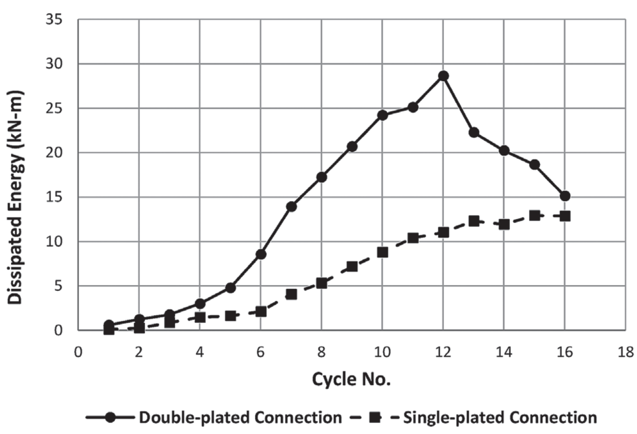

Fig. 27 *Variations in dissipated energy during cyclic loading*

jected to a series of scaled ground motions and cyclic loadings; their responses were evaluated and compared. The results of these analyses may be summarized as follows:

1- The modal analyses showed that the fundamental modes of vibration of the ODBS retrofitted frames have higher periods of vibration and a lower mass participation factor, which indicates that the number of effective modes participating in the response of frames retrofitted with ODBS is higher than those in the other bracing systems.

2- Under all the seismic excitations considered, the acceleration response of the ODBS was markedly lower than those of the other two bracing systems, which resulted in a much reduced base shear in the ODBS-retrofitted frames.

3- In terms of the acceleration response, the ODBS system performed best in seismic records containing higher frequency ranges. As the strong frequency range of the record decreases, the efficiency of the ODBS somewhat lessens, but always maintains its superior performance compared to the other bracing systems.

4- The results of the time history hysteresis response indicated that most of the buckling in the ODBS happened in a deformation range from $2\Delta_y$ to $4\Delta_y$, which is a much larger deformation range in comparison with the other bracing systems.

5- In both the time history and cyclic hysteresis response analyses, the ODBS system had the widest loops and largest area under the force-displacement curve, hence the most energy dissipation capacity compared to the other brace retrofitting systems.

6- In the X-braced RC frames, all the inelastic activities were, as expected, confined to the axial steel brace members, while the other structural members remained in an elastic range. On the other hand, in the frames retrofitted with ODBS, all the members participated in absorbing the energy.

7- In the RC frames retrofitted with ODBS, the dissipation of energy markedly increased at higher input loads. It was also noted that the ODBS dissipates more energy in the frames with smaller numbers of stories, which indicates that it is more effective in low-rise buildings.

8- Under cyclic loading, the slope of the energy dissipation-stiffness line for ODBS is markedly higher than the other retrofitting configurations, which indicates that the rate of increase in energy dissipation with increasing stiffness is more in the ODBS compared to the other retrofitting configurations.

9- It was shown that the double-plated central connection can control the adverse out-of-plane buckling response of the ODBS.

REFERENCES

Abou-Elfath, A., Ghobarah, A. (2000) *Behavior of reinforced concrete frames rehabilitated with concentric steel bracing*, Can. J. Civil Eng., 27: 433-444.

ACI 318 (2005) *Building Code Requirements for Structural Concrete (ACI 318-05)*, ACI Committee 318, American Concrete Institute, Farmington Hills, MI.

AISC (1999) *Load and resistance factor design specification for structural steel buildings*. Chicago, IL: American Institute of Steel Construction Inc (AISC), 1999.

AISC-05, ANSI/AISC 360 (2005) *Specification for structural steel buildings*, American Institute of Steel Construction, Chicago, 2005.

ASTM A595 / A595M-14 (2014) *Standard Specification for Steel Tubes, Low-Carbon or High-Strength Low-Alloy, Tapered for Structural Use*, ASTM International, West Conshohocken, PA, 2014.

Bazzaz, M., Andalib, Z., Kheyroddin, A., Kafi, M. A. (2015) *Numerical comparison of the seismic performance of steel rings in off-centre bracing system and diagonal bracing system*. Steel and Comp. Struct., 19(4):917-937.

Bush, T. D., Jones, E. A., Jirsa, J. O. (1991) *Behavior of RC frame strengthened using structural-steel bracing*. J Struct Eng-ASCE 1991; 117(4): 1115-26.

Chopra, A. K. (2016) *Dynamics of Structures*; Theory and Applications to Earthquake Engineering, Prentice Hall.

Ghaffarzadeh, H., Maheri, M. R. (2006) *Cyclic tests on the internally braced RC frames*, J. Seismology and Earthquake Engineering (JSEE); 8(3).

Hassan O. F., Goel S. C. (1991) *Modeling of bracing members and seismic behavior of concentrically braced steel structures*. Research Report UMCE 91-1. Ann Arbor, MI: Department of Civil Engineering, University of Michigan.

Khatib I. F., Mahin S. A., Pister K. S. (1988) *Seismic behavior of concentrically braced steel frames.* Report UCB/EERC-88/01. Berkeley, CA: Earthquake Engineering Research Center, University of California.

Lorenzo, D. S. L., Scotta R., Lazzari, M. (2015) *Optimal design of seismic retrofitting of RC frames with eccentric steel bracing*. Bull. Earthq. Eng., 13(2):613-633.

Maheri, M. R., Akbari, R. (2003) *Seismic behavior factor, R, for steel X-braced and knee-braced RC buildings*, Engineering Structures, 25(12): 1505-1513.

Maheri, M. R., Ghaffarzadeh, H. (2008) *Connection overstrength in steel-braced RC frames, Engineering Structures*, 30(7): 1938-1948.

Maheri, M. R., Kousari, R., Razazan, M. (2003) *Pushover tests on steel X-braced and knee-braced RC frames*. Eng Struct, 25(13): 1697-705.

Maheri, M. R., Sahebi, A. (1995) *Experimental investigation of the use steel bracing in reinforced concrete frames*. Proc. of 2nd Int. Conf. on Seism. Earthq. Eng., Tehran, Iran, Vol. 1, pp.755-784.

Maheri, M. R., Sahebi, A. (1997) *Use of steel bracing in reinforced concrete frames*. Eng Struct. 19(12): 1018-24.

Majidzamani, S., Rasouli, M. (2006) *Experimental investigation of behavior of Y-shaped concentric steel bracing.* Asian J. Civil Eng., 7(1):81-94.

Majidzamani, S., Vafaei, A., Aghakouchak, A. A., Desai, C. (2011) *Experimental investigation of steel frames braced with symmetrical pairs of y-shaped concentric bracings*. J. Steel Struct., 11(2):117-131.

Majidzamani, S., Vafaei, A., Desaib, C., Rasouli M. (2012) *Experimental investigation of behavior of steel frames with y-shaped concentric bracing*, Journal of Construct. Steel Res., 70:12–27.

Moghadam, H. A., Estekanchi, H. E. (1995) *On the characteristics of offcenter bracing system*, J Constr Steel Res, 35:361-76.

Moghadam, H. A., Estekanchi, H. E. (1999) *Seismic behavior of offcentre bracing system*, J Constr Steel Res, 51:177-96.

Ohishi, H., Takahashi, M., Yamazaki, Y. (1988) *A seismic strengthening design and practice of an existing reinforced concrete school building in Shizuoka city*, Proc. of 9th World Conference on Earthquake Engineering, Japan, VII, 415-420.

Ramin, K., Fereidoonfar, M. (2015) *Finite element modeling and nonlinear analysis for seismic assessment of off-diagonal steel braced RC frame*. Int. J. Concrete Struct. and Mat., 9(1):89-118.

Remennikov, A. M., Walpole, W. R. (1998) *Seismic behavior and deterministic design procedures for steel V braced frames*. Earthq Spectra, 14(2):335-55.

SAP2000 (ver15.0) (2015) *Software and manual*. Berkeley, CA: CSI: Computers and Structures Inc.

Sedaghati, P., Lotfollahi, M., Mofid, M. (2017) *Parametric study and design approach for off-center bracing system*, Struct. Design Tall Spec. Build. 26:e1311.

Tagawa, Y., Aoki, H., Huang, T., Masuda, H. (1992) *Experimental study of new seismic strengthening method for existing RC structure*, Proc. of 10th World Conference on Earthquake Engineering, Rotterdam, 5193-5198.

Tang, X., Goel, S. C. (1987) *Seismic analysis and design considerations of braced steel structures*. Research Report UMCE 87-4. Ann Arbor, MI: Department of Civil Engineering, University of Michigan.

Tasnimi, A., Masoomi, A. (1999) *Evaluation of response of reinforced concrete frames strengthened with steel bracing*. Proceedings of the Third International Conference on Seismology and Earthquake Engineering, Iran.